Doxorubicin induces arterial stiffness : a comprehensive in vivo and ex vivo evaluation of vascular toxicity in mice

Doxorubicin induces arterial stiffness: a comprehensive *in vivo* and *ex vivo* evaluation of vascular toxicity in mice

Matthias Bosman[1], Kasper Favere[1, 2, 3, 4], Cédric H.G. Neutel[1], Griet Jacobs[1], Guido R.Y. De Meyer[5], Wim Martinet[5], Emeline M. Van Craenenbroeck[2, 4] and Pieter-Jan D.F. Guns[1]

[1] University of Antwerp, Faculty of Medicine and Health Sciences, Laboratory of Physiopharmacology, Campus Drie Eiken, Universiteitsplein 1, B-2610, Antwerp, Belgium

[2] University of Antwerp, Research Group Cardiovascular Diseases, GENCOR, Antwerp, Belgium

[3] Ghent University, Faculty of Medicine and Health Sciences, Department of Internal Medicine, C. Heymanslaan 10, B-9000, Ghent, Belgium

[4] Antwerp University Hospital (UZA), Department of Cardiology, Drie Eikenstraat 655, B-2650, Edegem, Belgium

[5] University of Antwerp, Faculty of Pharmaceutical, Biomedical and Veterinary Sciences, Laboratory of Physiopharmacology, Campus Drie Eiken, Universiteitsplein 1, B-2610, Antwerp, Belgium

Corresponding author: Matthias Bosman: University of Antwerp, Faculty of Medicine and Health Sciences, Laboratory of Physiopharmacology, Campus Drie Eiken, Universiteitsplein 1, B-2610, Antwerp, Belgium. E-mail: matthias.bosman@uantwerpen.be

Funding information: M.B., K.F. and C.N. are predoctoral fellows of the Fund for Scientific Research (FWO) Flanders [grant number: 1S33720N, 11C6321N and 1S24720N, respectively]. E.V.C. is holder of a senior clinical investigator grant from FWO Flanders [grant number: 1804320N]. Furthermore, the research is supported by a DOCPRO4 grant of the Research Council of the University of Antwerp (ID: 39984) and by the INSPIRE project, which has received funding from the European Union's Horizon 2020 Research and Innovation Program (H2020-MSCA-ITN program, Grant Agreement: No858070).

Figure 5 & 7 are preferably displayed in colour online; all other figures can be shown in greyscale.

ABBREVIATIONS

aaPWV = abdominal aorta pulse wave velocity

ACh = acetylcholine

cfPWV = carotid – femoral pulse wave velocity

DEANO = diethylamine NONOate

DOX = doxorubicin

EC(s) = endothelial cell(s)

eNOS = endothelial nitric oxide synthase

L-NAME = Nω-nitro-L-arginine methyl ester

LVEF = left ventricular ejection fraction; LVAW = left ventricular anterior wall; LVID = left ventricular internal diameter; LVPW = left ventricular posterior wall

NO = nitric oxide

PE = phenylephrine

ROTSAC = Rodent Oscillatory Tension Set-up to study Arterial Compliance

VSMC(s) = vascular smooth muscle cell(s)

ABSTRACT

Arterial stiffness is an important predictor of cardiovascular risk. Clinical studies have demonstrated that arterial stiffness increases in cancer patients treated with the chemotherapeutic doxorubicin (DOX). However, the mechanisms of DOX-induced arterial stiffness remain largely unknown. This study aimed to evaluate artery stiffening in DOX-treated mice using *in vivo* and *ex vivo* techniques. Male C57BL/6J mice were treated for 2 weeks with 2 mg/kg (low dose) or 4 mg/kg (high dose) of DOX weekly. Arterial stiffness was assessed *in vivo* with ultrasound imaging (abdominal aorta pulse wave velocity (aaPWV)) and applanation tonometry (carotid-femoral PWV) combined with *ex vivo* vascular stiffness and reactivity evaluation. The high dose increased aaPWV, while cfPWV did not reach statistical significance. Phenylephrine (PE)-contracted aortic segments showed a higher Peterson's modulus (Ep) in the high dose group, while Ep did not differ when vascular smooth muscle cells (VSMCs) were relaxed by a NO donor (DEANO). In addition, aortic rings of DOX-treated mice showed increased PE contraction, decreased basal nitric oxide (NO) index and impaired acetylcholine-induced endothelium-dependent relaxation. DOX treatment contributed to endothelial cell loss and reduced endothelial nitric oxide synthase (eNOS) expression in the aorta. In conclusion, we have replicated DOX-induced arterial stiffness in a murine model and this aortic stiffness is driven by impaired endothelial function, contributing to increased vascular tone.

KEY WORDS

Arterial stiffness, doxorubicin, endothelial dysfunction, cardio-oncology, cardiovascular toxicity

1. INTRODUCTION

Large artery stiffening is an important feature in the process of vascular ageing [1, 2]. Under physiological conditions, the heart ejects blood from the left ventricle into the aorta at high velocity [2]. The distensibility of the aorta during systole will mitigate the increase in aortic pressure, while the elastic recoil during diastole supports blood flow [3-5]. In contrast, arterial stiffening impairs the dampening capacity of the aorta, which, in turn, leads to increased afterload on the heart and increased pulsatility in highly perfused organs, such as the kidneys, brain and heart, potentially damaging them [6]. In previous studies, stiffening of the aorta has been associated with increased risk of developing coronary artery disease, atrial fibrillation, stroke and heart failure [7-9]. Hence, arterial stiffness, measured non-invasively by pulse wave velocity (PWV), is an early and predictive marker of future cardiovascular events [10].

For a long time, research has mainly focussed on structural changes contributing to arterial stiffness, such as the balance between collagen synthesis and elastin degradation within the vascular wall [11-13]. Although structural remodelling is an important contributor to vascular ageing, there is emerging evidence that artery stiffening is regulated by active components as well. More specifically, endothelial cells (ECs) and vascular smooth muscle cells (VSMCs) have been reported to contribute to arterial stiffness by dysregulating vascular tone [14, 15]. For example, decreased nitric oxide (NO) bioavailability and elevated contraction are associated with increased aortic stiffness [16, 17]. Therefore, large artery stiffening depends on a delicate, not mutually exclusive, balance between these active and passive elements.

In humans, carotid-femoral pulse wave velocity (cfPWV) assessed by tonometry is the gold-standard method for evaluating arterial stiffness, but in mice ultrasound imaging is more frequently used [18, 19]. Ultrasound imaging offers a local determination of aorta PWV, such as abdominal aorta PWV (aaPWV) [20], while tonometry focusses more on regional determination of PWV [21]. These *in vivo* techniques offer a high translational value, but do not provide insight about the underlying active and passive mechanisms that are involved. In addition, *in vivo* measurements are dependent on heart rate and blood pressure [22]. Therefore, we have established a unique in-house developed organ bath set-up, called the Rodent Oscillatory Tension Set-up to study Arterial Compliance (ROTSAC), to assess arterial stiffness *ex vivo*, independent from confounding factors, such as heart rate and blood pressure [17, 23, 24].

Here we present a preclinical study investigating arterial stiffness in mice treated with doxorubicin (DOX). DOX is a chemotherapeutic of the class of anthracyclines that is used to treat a wide variety of cancers, such as breast cancer, lymphoma and haematological malignancies [25]. However, dose-dependent cardiotoxicity limits the clinical use of DOX [26]. The mechanisms of DOX-induced cardiotoxicity have been intensively investigated (reviewed elsewhere) [26], yet the effects on the vascular system have been less considered. Clinical studies have shown increased arterial stiffness after DOX-therapy. Moreover, some childhood cancer survivors show signs of accelerated cardiovascular ageing as well [27-30]. In murine models, DOX contributes to EC and VSMC dysfunction [31, 32]. More specifically, DOX mediates excessive reactive oxygen species (ROS) production, which might impair NO signalling, thereby disturbing endothelium-dependent vasodilation *ex vivo* [33]. Furthermore, low doses of DOX induce senescence of VSMCs *in vitro*, contributing to vascular damage [34]. However, it remains unclear whether increased arterial stiffness in DOX-treated patients is caused by an altered vascular tone or by structural remodelling. Therefore, the current study aimed to replicate DOX-induced arterial stiffening in a preclinical murine model and to delineate the mechanisms involved herein.

2. MATERIALS & METHODS

2.1 Animals & Ethical approval

24 male C57BL/6J mice (Charles River, France) between an age of 10 and 12 weeks and with a body weight between 26 and 30 g were housed in the animal facility of the University of Antwerp in standard cages with 12-12 hours light-dark cycles with access to regular chow and water *ad libitum*. Male mice were chosen to avoid the influence of female hormone confounding factors. The experiments were approved by the Ethical Committee of the University of Antwerp and were conform to the ARRIVE guidelines and to the Guide for the Care and Use of Laboratory Animals published by the US National Institutes of Health (NIH Publication no.85-23, revised 1996).

2.2 DOX treatment and experimental workflow

Mice were randomly divided into three groups: vehicle (n = 8), low dose DOX (2 mg/kg; n = 8) and high dose DOX (4 mg/kg; n = 8). DOX was injected intraperitoneally once per week for a total of two weeks. DOX (Adriamycin®, 2 mg/mL) was diluted in a 0.9% NaCl solution (B. Braun, Belgium) on the day of injection. The vehicle group received an intraperitoneal injection (10 mL/kg) of a 0.9% NaCl solution. Ultrasound imaging was performed before (day -1) and 4, 7 and 11 days after the start of DOX treatment. The time points were selected based on a pilot study where mice were measured daily after treatment with a high dose of DOX (data not shown). Applanation tonometry and blood pressure were evaluated on day 5 and 10, respectively, after starting DOX treatment. Mice were sacrificed between 12 and 13 days after the start of treatment for *ex vivo* measurements with ROTSAC and organ baths. Supplementary figure 1 provides an overview of the experimental design and workflow.

2.3 High-frequency ultrasound imaging

Ultrasound imaging was performed in anaesthetised mice under 1.5 - 2.5% (v/v) isoflurane (Forene; Abbvie, Belgium) using a high-frequency ultrasound system (Vevo2100, VisualSonics). Images were only acquired when heart rate and body temperature met the inclusion criteria, i.e. 550 ± 50 beats/min and 37 ± 1 °C, respectively. M-mode images were obtained for determination of cardiac parameters using a 24-MHz transducer. Left ventricular ejection fraction (LVEF), left ventricular internal diameter (LVID), stroke volume, left ventricular anterior wall (LVAW) and left ventricular posterior wall (LVPW) thickness were subsequently calculated using measurements of three consecutive M-mode cycles with Vevo LAB Software (Version 3.2.0, VisualSonics). In the same session, abdominal aorta PWV (aaPWV) was determined according to the method developed by Di Lascio et al. with a 24-MHz transducer [20]. Briefly, pulse wave Doppler tracing was used to measure aortic flow velocity (V).

Immediately thereafter, aortic diameter (D) was measured on 700 frames-per-second B-mode images of the abdominal aorta in EKV imaging mode. The ln(D)-V loop method was then applied to calculate aaPWV, using MathLab v2014 software (MathWorks).

2.4 Applanation tonometry

Carotid-femoral PWV (cfPWV) was determined in anaesthetised mice (4 - 6% sevoflurane (v/v) (Sevorane; Abbvie, Belgium), as previously described by our research group [21]. In brief, two pulse tonometers (SPT-301, Millar Instruments) were applied on the skin using a micromanipulator. Carotid–femoral transit time (Δt) was determined using the time difference between the foot of carotid and femoral artery pulses (foot-to-foot method). The foot of the pressure wave was defined as the second derivative maximum. Fifty consecutive pulses with sufficient amplitude and a reproducible waveform were analysed; pulses that interfered with respiratory movement peaks were excluded.

2.5 Blood pressure evaluation

Systolic and diastolic blood pressure were determined at day 10 non-invasively in restrained, awake mice using a tail-cuff system with programmed electrosphygmomanometer (Coda, Kent Scientific Corporation). To reduce stress and variability during the procedure, animals were trained for two days prior to the actual measurements.

2.6 *Ex vivo* evaluation of aortic stiffness and vascular reactivity

Mice were intraperitoneally injected with sodium pentobarbital (75 mg/kg; Sanofi, Belgium), followed by perforation of the diaphragm (when under deep anaesthesia). The thoracic aorta was carefully dissected and cut into six segments of 2 mm length (i.e. TA0 to TA5) with the crossing of the diaphragm as the reference point for the sixth segment (TA5). Next, segments were mounted between two hooks of an *ex vivo* organ bath set-up (10 mL) filled with Krebs Ringer solution (37°C, 95% O2/5% CO2, pH 7.4) containing (in mmol/L): NaCl 118, KCl 4.7, CaCl2 2.5, KH2PO4 1.2, MgSO4 1.2, NaHCO3 25, CaEDTA 0.025, and glucose 11.1.

For ROTSAC: *Ex vivo* assessment of arterial stiffness was performed as previously described [23]. In brief, segments (TA2 and TA3) were continuously stretched between alternating preloads corresponding to “systolic” and “diastolic” transmural pressures and at a physiological frequency of 10 Hz to mimic the physiological heart rate in mice (600 beats/ min). The set-up is calibrated by acquiring photographs of each aorta segment at different tensions (10 to 60 mN), from which the diameter and width of the segment are determined. Subsequently, these parameter serve as input in the LaPlace’s equation to calculate in real-time the “systolic” and “diastolic” pressure

and the Peterson's modulus (Ep), a measure for arterial stiffness. Ep was calculated as follows: $Ep = D_0 * \Delta P/\Delta D$ with ΔP = difference in pressure (kept constant at 40 mmHg), D_0 = "diastolic" diameter and ΔD = the change in diameter between "diastolic" and "systolic" pressure.

The ROTSAC protocol included the evaluation of arterial stiffness (Ep) at different pressures (i.e. 60-100, 80-120, 100-140 and 120-160 mmHg). Furthermore, the contribution of VSMC tonus was investigated by adding a high concentration (2 µM) of the α1-adrenergic receptor agonist phenylephrine (PE), while the contribution of ECs was evaluated by blocking endothelial nitric oxide synthase (eNOS) with Nω-nitro-L-arginine methyl ester (L-NAME, 300 µM). Conversely, a high concentration (2 µM) of the NO-donor diethylamine NONOate (DEANO) was added to completely relax VSMCs to remove vascular tonus, which allows the evaluation of passive stiffness of the vessel wall. The detailed protocol for the ROTSAC experiments is provided in supplementary figure 2.

For organ baths with isometric transducer: aortic segments (TA4 and TA5) were mounted at a preload of 20 mN. Since we have previously shown that basal NO declines over time [35], the experimental protocol was started 70 minutes after puncture of the diaphragm to minimise time-dependent biases. VSMC contraction was evaluated by adding cumulative concentrations of PE (3 nM – 10 µM). Additionally, the basal NO index was calculated as follows: PE was first added to induce VSMC contraction (PE contraction). Once the contraction was stable, the eNOS blocker L-NAME (PE + L-NAME contraction) was subsequently added, further increasing contraction. By substracting the PE contraction from the PE + L-NAME contraction, the amount of contraction that is solely due to L-NAME (eNOS inhibition) can be acquired, which provides an estimate of basal NO. Endothelium-dependent relaxation was investigated by addition of cumulative concentrations of acetylcholine (ACh), a muscarinic receptor agonist. The involvement of Ca^{2+}-channels was determined by adding a single, high concentration (35 µM) of diltiazem, a voltage-gated Ca^{2+}-channel blocker. The detailed protocol for the organ bath experiments and the method for basal NO index calculation is illustrated in supplementary figure 3.

2.7 Chemical compounds

DOX (Adriamycin®, 2 mg/mL) was purchased from Pfizer (Belgium). PE, L-NAME, ACh, DEANO and diltiazem were purchased from Sigma-Aldrich (Belgium).

2.8 Histology

Aortic segments were fixed in 4% formalin for 24 h, dehydrated overnight in 60% isopropanol and then embedded in paraffin. Transversal sections were stained with orcein or immunohistochemically stained with a primary antibody against collagen type I (1:500; ab21286, Abcam) to determine elastin and collagen type I content, respectively. The EC layer continuity was evaluated with immunohistochemical staining with a primary antibody against CD31 (1:100; D8V9E, Cell Signalling Technology) and visualised with EnVision+ (Dako). Images were acquired with Universal Graph 6.1 software using an Olympus BX40 microscope and quantified with ImageJ software. Elastin and collagen type I content were quantified by calculating the signal-to-wall area ratio (expressed as percentage). CD31 was quantified by determining the length of CD31 positive cells along the luminal border divided by the total aortic lumen circumference (expressed as percentage).

2.9 Western blotting

Aortic samples were lysed in Laemmli sample buffer (Bio-Rad) containing 5% β-mercaptoethanol (Sigma-Aldrich) and subsequently heat-denatured for 5 minutes at 100 °C. Next, samples were loaded on Bolt 4–12% Bis-Tris gels (Invitrogen) and after electrophoresis transferred to Immobilon-FL PVDF membranes (Millipore) according to standard procedures. Thereafter, membranes were immediately blocked for 1 hour in Odyssey Li-COR blocking buffer. After blocking, membranes were probed with primary antibodies, diluted in Odyssey Li-COR blocking buffer, overnight at 4 °C. The following primary antibodies were used: mouse anti-eNOS (1:500; ab76198, Abcam) and mouse anti-β-actin (1:5000; ab8226, Abcam). The next day, membranes were incubated with IRDye-labeled secondary antibodies (goat anti-rabbit IgG926-32211; goat anti-mouse IgG926-68070, both purchased from Li-COR Biosciences) for 1 hour at room temperature. Membranes were visualised with an Odyssey SA infrared imaging system (Li-COR Biosciences). Western blot data was quantified using ImageJ software. Signal intensity of the protein of interest (eNOS) was normalised to the β-actin signal intensity and expressed as the fold change (compared to vehicle).

2.10 Statistical analysis

All results were expressed as the mean ± standard error of the mean (SEM). Statistical analyses were performed using GraphPad Software (Prism 8 - Version 8.4.2, Graphpad, USA). Repeated measures two-way ANOVA, one-way ANOVA and Kruskal-Wallis tests were performed for comparison between groups. A Dunnett's post hoc test was used to correct for multiple comparisons. A Bland-Altman plot was used to evaluate concordance between aaPWV (day 4 and 7) and cfPWV (day 5) values. A p-value < 0.05 was considered to be statistically significant.

3. RESULTS

3.1 DOX (high dose) increased aaPWV *in vivo*

A significant and consistent increase in aaPWV was observed for the high dose group at 4, 7 and 11 days after the start of DOX treatment (Figure 1A). More specifically, at 4, 7 and 11 days, aaPWV was 5.67 ± 0.32 m/s, 5.36 ± 0.30 m/s and 5.034 ± 0.25 m/s in the high dose group compared to 4.36 ± 0.31 m/s, 4.00 ± 0.24 m/s and 4.13 ± 0.20 m/s in the vehicle group, respectively (Figure 1A). LVEF did not differ among treatment groups (Figure 1B). Additional evaluated cardiovascular parameters, including LVAW, LVID, LVPW, stroke volume, heart mass and body weight (measured at day 11) are provided in Table 1. These parameters did not change between the different treatment groups after DOX treatment (Table 1), except pulse pressure. Pulse pressure, the difference between systolic and diastolic blood pressure, was significantly elevated in the high dose group (Table 1).

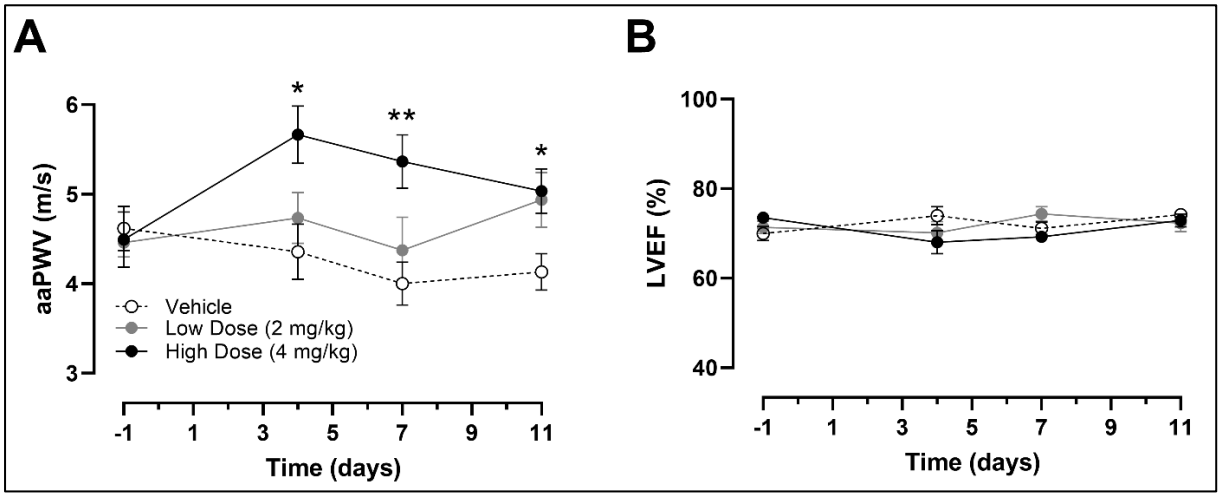

Figure 1: *In vivo* measurement of aaPWV and LVEF in vehicle-, low dose- and high dose-treated mice. High dose treatment of DOX increased aaPWV significantly compared to the vehicle group at 4, 7 and 11 days after the start of DOX treatment (A). LVEF did not change during treatment among all groups (B). For vehicle: n = 8, low dose: n = 8 and high dose: n = 8. For A & B: Repeated measures two-way ANOVA with Dunnett's multiple comparisons test. *, ** $p < 0.05$, 0.01. (2-column fitting image)

Table 1: Additional cardiovascular parameters and body weight.

	Vehicle	Low Dose (2 mg/kg)	High Dose (4 mg/kg)
LVAW thickness systole (mm)	1.20 ± 0.07	1.20 ± 0.05	1.19 ± 0.04
LVAW thickness diastole (mm)	0.78 ± 0.03	0.76 ± 0.03	0.77 ± 0.03
LVID systole (mm)	1.86 ± 0.06	1.90 ± 0.12	2.05 ± 0.06
LVID diastole (mm)	3.33 ± 0.07	3.18 ± 0.13	3.48 ± 0.06
LVPW thickness systole (mm)	1.50 ± 0.07	1.46 ± 0.03	1.53 ± 0.04
LVPW thickness diastole (mm)	0.91 ± 0.05	0.96 ± 0.08	0.90 ± 0.03
Stroke volume (µL)	33.8 ± 1.73	29.3 ± 2.27	36.65 ± 1.64
Heart mass (mg)	143.2 ± 6.1	139.9 ± 1.9	133.7 ± 4.4
Body weight (g)	27.8 ± 0.8	27.2 ± 0.9	25.8 ± 0.8
Systolic blood pressure (mmHg)	103 ± 4	104 ± 4	105 ± 3
Diastolic blood pressure (mmHg)	77 ± 3	74 ± 5	72 ± 3
Pulse pressure (mmHg)	26 ± 2	30 ± 1	33 ± 2 *

Abbreviations: LVAW, left ventricular anterior wall; LVID, left ventricular internal diameter; LVPW, left ventricular posterior wall. * $p < 0.05$ compared to vehicle. For vehicle: n = 8, low dose: n = 8 and high dose: n = 8. (2-column fitting table)

Measurement with tonometry, only performed at day 5 for logistical reasons, showed a trend (p = 0.0547) of increased cfPWV in the high dose group (Figure 2A). Individual aaPWV-values for all time points are presented in Figure 2B to illustrate inter-animal variability. To evaluate the agreement between aaPWV and cfPWV measurement techniques a Bland-Altman plot was created. Bland-Altman analysis revealed that aaPWV values were systematically higher than cfPWV values (bias = 1.372) (Figure 2C). In addition, the bias tended to be higher with increasing PWV values (Figure 2C).

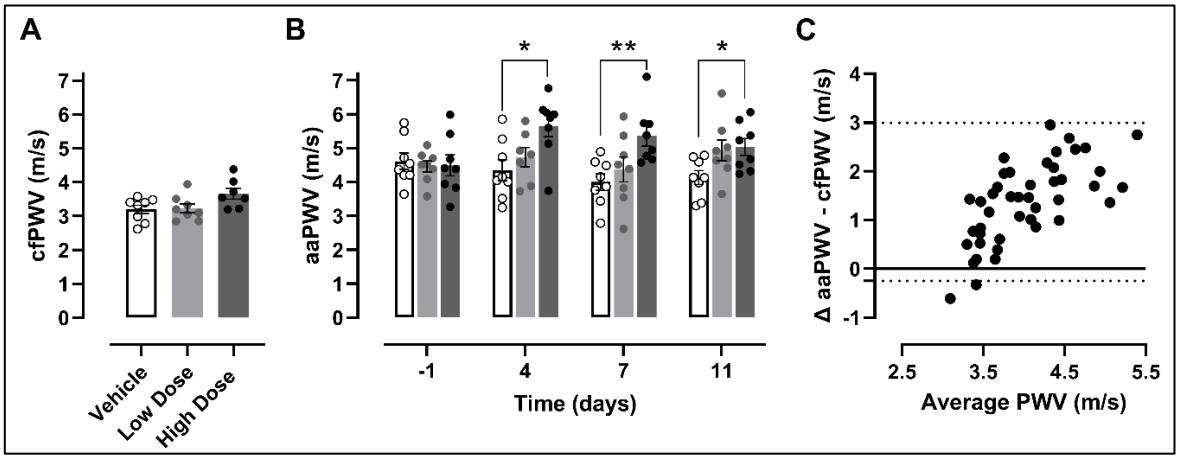

Figure 2: *In vivo* measurement of cfPWV in vehicle-, low dose- and high dose-treated mice and comparison of aaPWV and cfPWV. cfPWV in the high dose group did not significantly increase compared to the vehicle group (p = 0.0547) (A). aaPWV values were systematically higher than cfPWV values after Bland-Altman analysis (bias = 1.372) (B & C). For vehicle: n = 8, low dose: n = 8 and high dose: n = 8. For A: One-way ANOVA with Dunnett's multiple comparisons test. For B: Repeated measures two-way ANOVA with Dunnett's multiple comparisons test. For C: Bland-Altman graph (dotted lines represent 95% limits of agreement) *, ** p < 0.05, 0.01. (2-column fitting image)

3.2 DOX (high dose) increased aortic stiffness *ex vivo*

The "diastolic" and "systolic" diameters (at 80 –120 mmHg) in Krebs Ringer and PE conditions, determined in the *ex vivo* ROTSAC set-up, are presented in figure 3A and 3B, respectively. The change (Δ) in "systolic" and "diastolic" diameter after PE-addition as compared with Krebs Ringer conditions was calculated (Figure 3C). This Δ diameter corresponds with the magnitude of contraction. In the high dose group, the change in "systolic" and "diastolic" diameter increased significantly, reflecting higher PE-induced contractions. Low dose-treated animals showed a non-significant trend towards elevated contraction (Figure 3C).

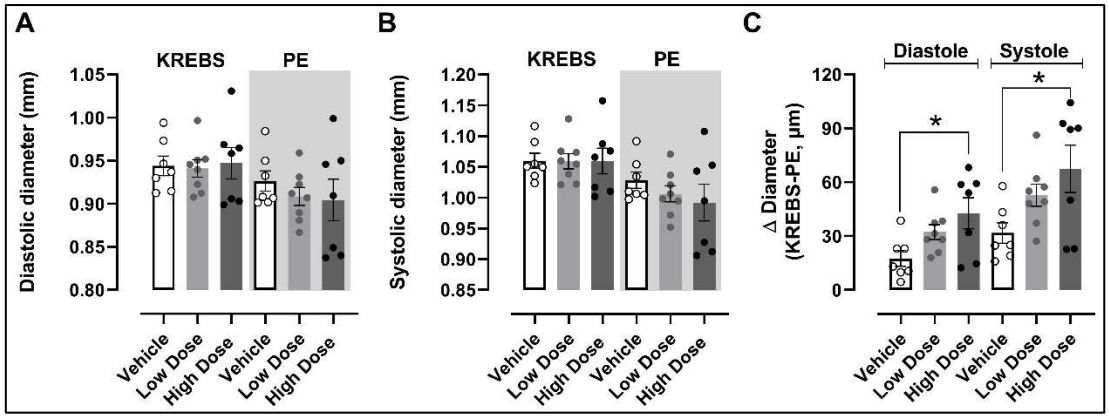

Figure 3: Evaluation of "diastolic" and "systolic" diameters in the *ex vivo* ROTSAC set-up. Diastolic and systolic diameter in Krebs Ringer and PE conditions at 80-120 mmHg (A & B). Δ Diameter (Krebs - PE) was significantly increased in high dose-treated mice during systole and diastole (C). For vehicle: n = 8, low dose: n = 8 and high dose: n = 7. For C: One-way ANOVA with Dunnett's multiple comparisons test. * $p < 0.05$ (2-column fitting image)

Ep, a measure of arterial stiffness, showed a pressure-dependent increase in all groups. Under Krebs Ringer conditions, there was no significant difference in Ep between vehicle- and DOX-treated mice, both in the absence and presence of L-NAME (300 µM) (Figure 4A & 4B). Similarly, in the presence of DEANO (2 µM), a NO-donor that removes vascular tonus, there were no differences in Ep between the vehicle and DOX-treated groups (Figure 4C), indicating no alteration in passive stiffness. However, Ep was significantly increased in the high dose-treated mice as compared with the vehicle-treated mice when aortic rings were stimulated with PE (2 µM) (Figure 4D). Mice treated with the low dose of DOX did not exhibit a higher Ep value in the presence of PE (Figure 4D). Remarkably, the high dose of DOX did not show a pressure-dependent increase in Ep in the combined presence of PE and L-NAME. More specifically, mice treated with the high dose of DOX exhibited a lower Ep value at 120 - 160 mmHg compared to the vehicle group (Figure 4E).

Furthermore, we determined the basal NO index by calculating the increase in Ep due to inhibition of eNOS with L-NAME (Supplementary figure 2). The basal NO index (at 80-120 mmHg) was significantly decreased in the high dose group as compared with the vehicle group (Figure 4F).

Finally, histological staining for elastin and collagen type I visualisation in aorta samples was performed to investigate potential structural remodelling (Figure 5). Elastin (Figure 5A) and collagen type I (Figure 5B) content did not differ between the treatment groups.

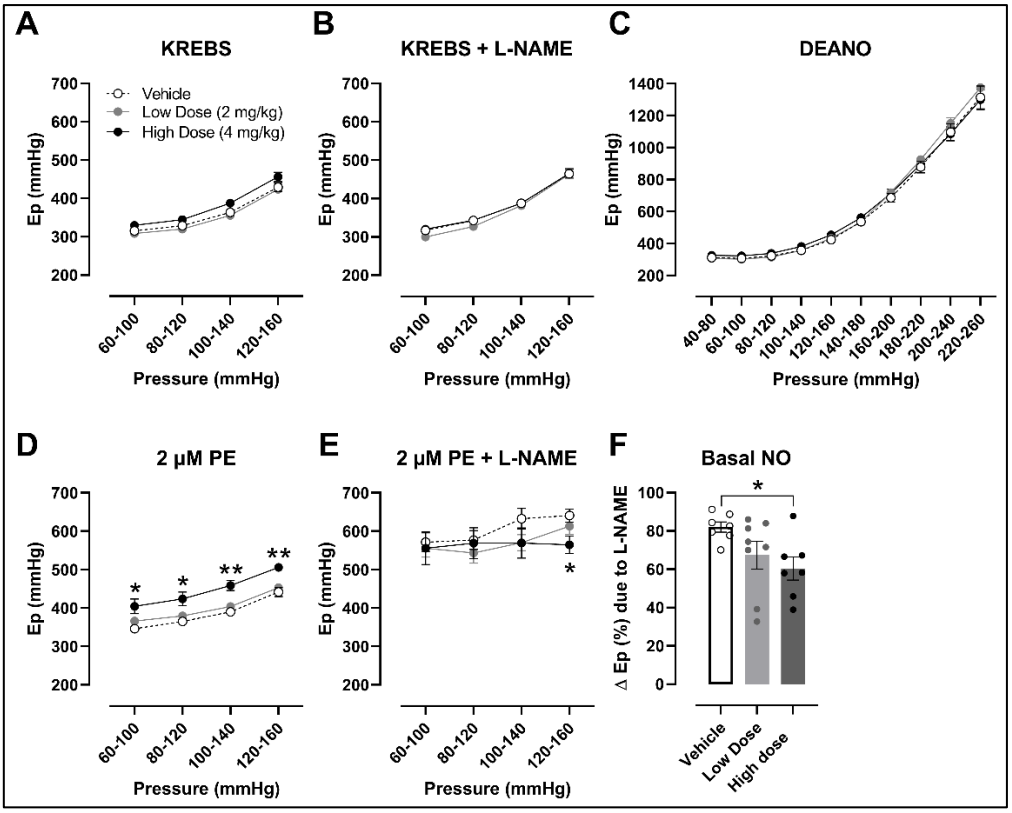

Figure 4: Assessment of aortic stiffness in mice treated with vehicle, low and high dose of DOX at different pressures with the *ex vivo* ROTSAC set-up. Peterson's modulus (Ep), a measure for aortic stiffness, did not significantly differ between vehicle- and DOX-treated mice in Krebs conditions in the absence and presence of L-NAME (A &B). Ep was similar in all treatment groups in the presence of DEANO (C). Addition of 2 µM PE increased Ep in the high dose group compared to the vehicle group (D). In the presence of PE (2 µM) combined with L-NAME (300 µM), the high dose group showed no pressure-dependency of Ep, resulting in a lower Ep at 120–160 mmHg (E). Basal NO index was significantly reduced the high dose group (F). For vehicle: n = 8, low dose: n = 8 and high dose: n = 7. For A-E: Repeated measures two-way ANOVA with Dunnett's multiple comparisons test. For F : One-way ANOVA with Dunnett's multiple comparisons test. *, ** $p < 0.05$, <0.01 (2-column fitting image)

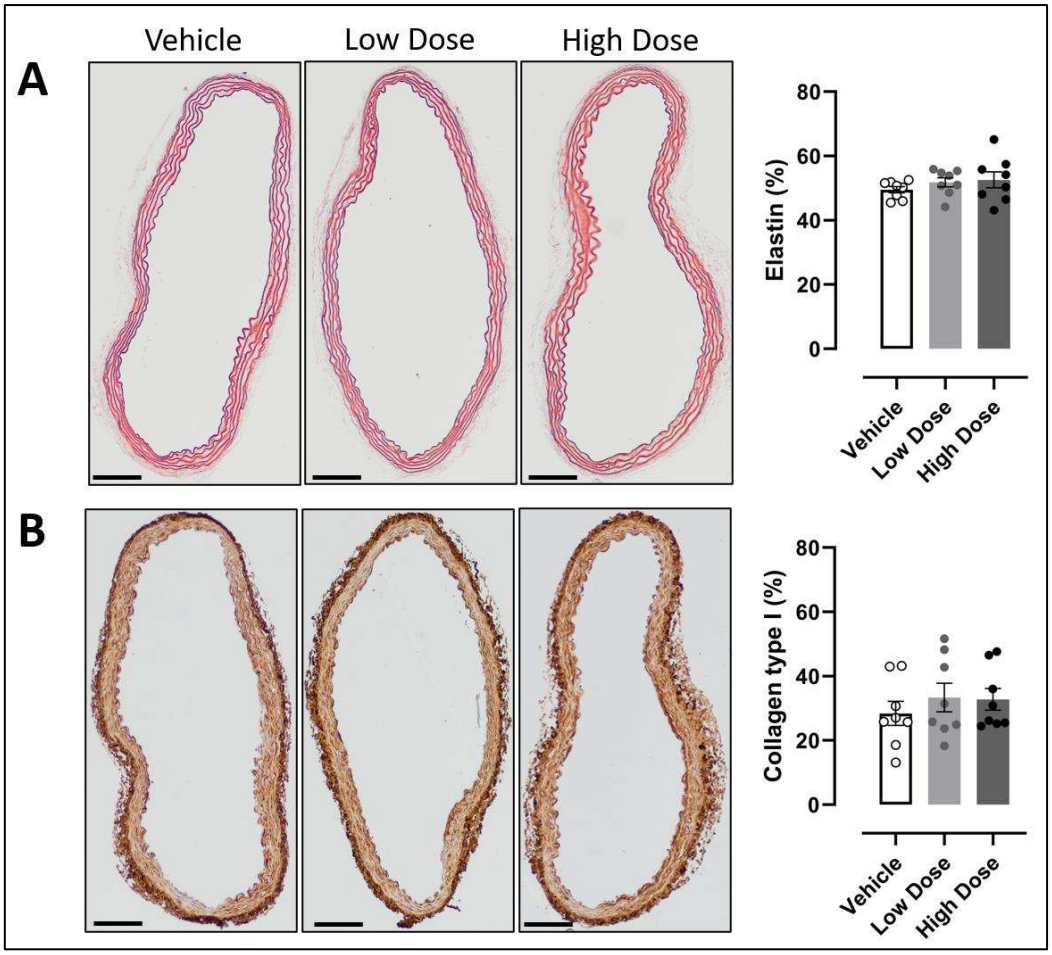

Figure 5: Evaluation of elastin and collagen type I content in the aortic wall of mice treated with vehicle, low and high dose of DOX. The elastin (A) and collagen type I (B) amount were not altered in the different treatment groups. For vehicle: n = 8, low dose: n = 8 and high dose: n = 8. For A and B: One-way ANOVA with Dunnett's multiple comparisons test ($p > 0.05$ for low and high dose compared to vehicle). Scale bar: 100 µM. (2-column fitting image)

3.3 DOX impaired endothelium-dependent relaxation, basal NO index and increased contraction

The high dose group exhibited increased PE-induced contractions compared to the vehicle, while the low dose did not (Figure 6A). This difference disappeared in the presence of L-NAME (Figure 6A). The sensitivity of VSMCs for PE (defined by the EC_{50}) was significantly elevated in animals treated with the high dose of DOX (Figure 6B). More specifically, the mean EC_{50}-values (logarithmic) were -7.014 ± 0.050 M and -6.796 ± 0.052 M for the high dose and vehicle groups, respectively.

We further determined the basal NO index by calculating the change in isometric force due to eNOS-inhibition with L-NAME (Supplementary figure 3). The basal NO index was significantly decreased in the high dose group as compared with the vehicle group (Figure 6C).

ACh-induced endothelium-dependent relaxation was impaired (Figure 6D). Both the maximal relaxation and the sensitivity for ACh was significantly reduced in the high dose-treated mice (Figure 6D & 6E). More specifically,

the mean EC_{50}-values (logarithmic) were -7.454 ± 0.073 M and -7.751 ± 0.086 M for the high dose and vehicle groups, respectively. In addition, there was no difference in DEANO-induced endothelium-independent relaxation between vehicle and DOX-treated mice nor in the sensitivity of VSMCs for DEANO (Figure 6D). For diltiazem (35 µM), no differences in the magnitude of relaxation were present between the different groups (Figure 6F).

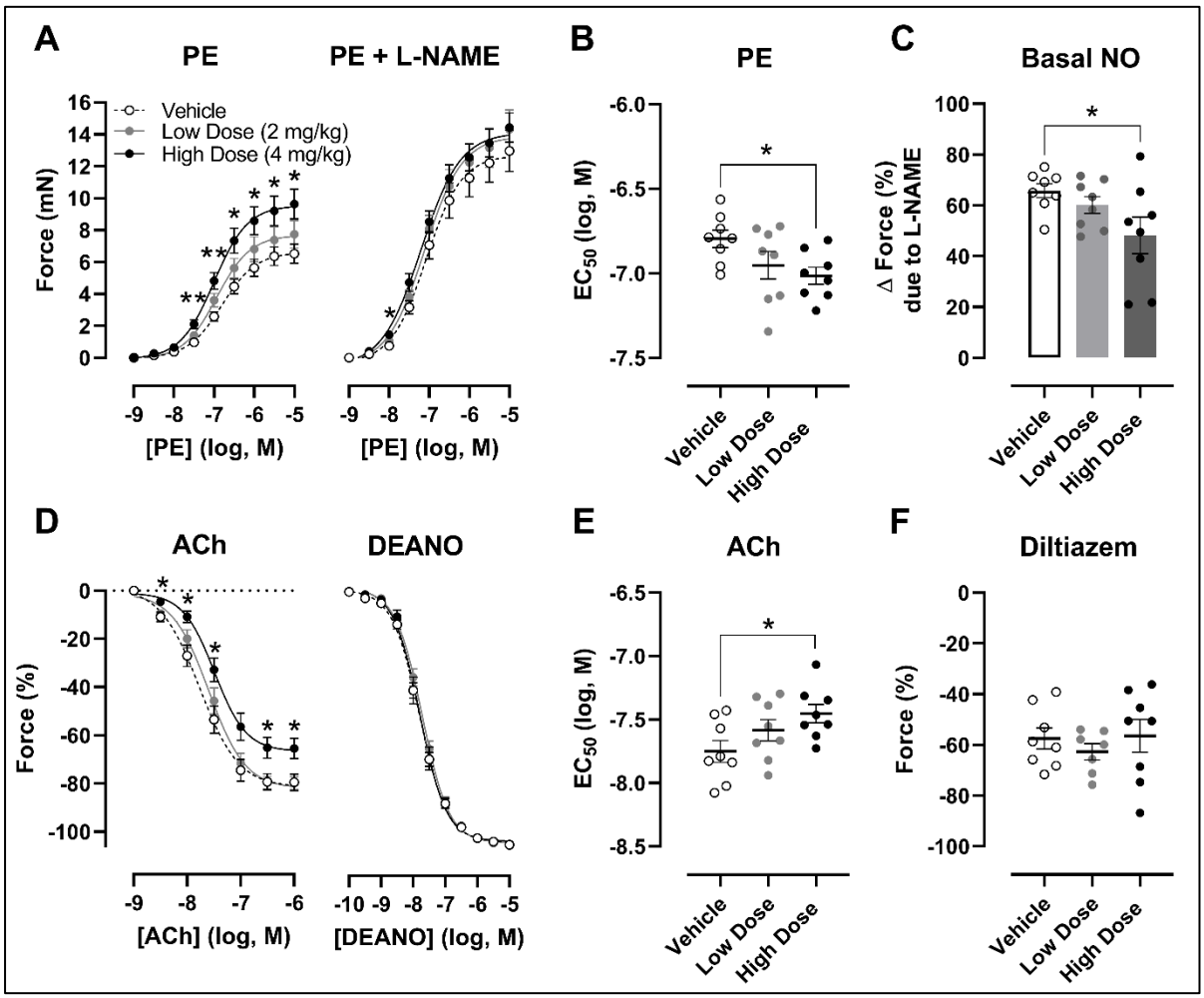

Figure 6: VSMC and EC function in mice treated with vehicle, low and high dose of DOX determined in organ baths with isometric force transducer. Concentration-response curves for mice treated with vehicle, low and high dose of DOX under PE-stimulation in the absence and presence of L-NAME (A), ACh (D) and DEANO (D). Contraction and VSMC-sensitivity for PE increased significantly in high dose-treated mice compared to vehicle group (A & B), but not after addition of L-NAME (A). Basal NO index, calculated from panel A, was significantly reduced in high-dose treated mice (C). No changes were present in the magnitude of DEANO-induced relaxation (D). ACh-induced relaxation and sensitivity of the endothelium for ACh decreased significantly in the high dose group (D & E). Diltiazem-induced relaxation did not differ between treatment groups (F). For vehicle: n = 8, low dose: n = 8 and high dose: n = 8. For A and D: Repeated measures two-way ANOVA with Dunnett's multiple comparisons test. For B, C, E and F: One-way ANOVA with Dunnett's multiple comparisons test. *, ** $p < 0.05$, <0.01 (2-column fitting image)

3.4 DOX disrupted EC layer continuity and decreased eNOS-expression

Endothelial layer continuity and eNOS-expression in the aorta were further investigated. The EC layer was evaluated with an immunohistochemical stain against CD31, a marker for ECs. CD31 positivity was significantly

decreased in the high dose group compared to the vehicle in a dose-dependent way, revealing gaps in the EC monolayer (Figure 7A). In addition, eNOS-expression was reduced in the high dose group as well (Figure 7B).

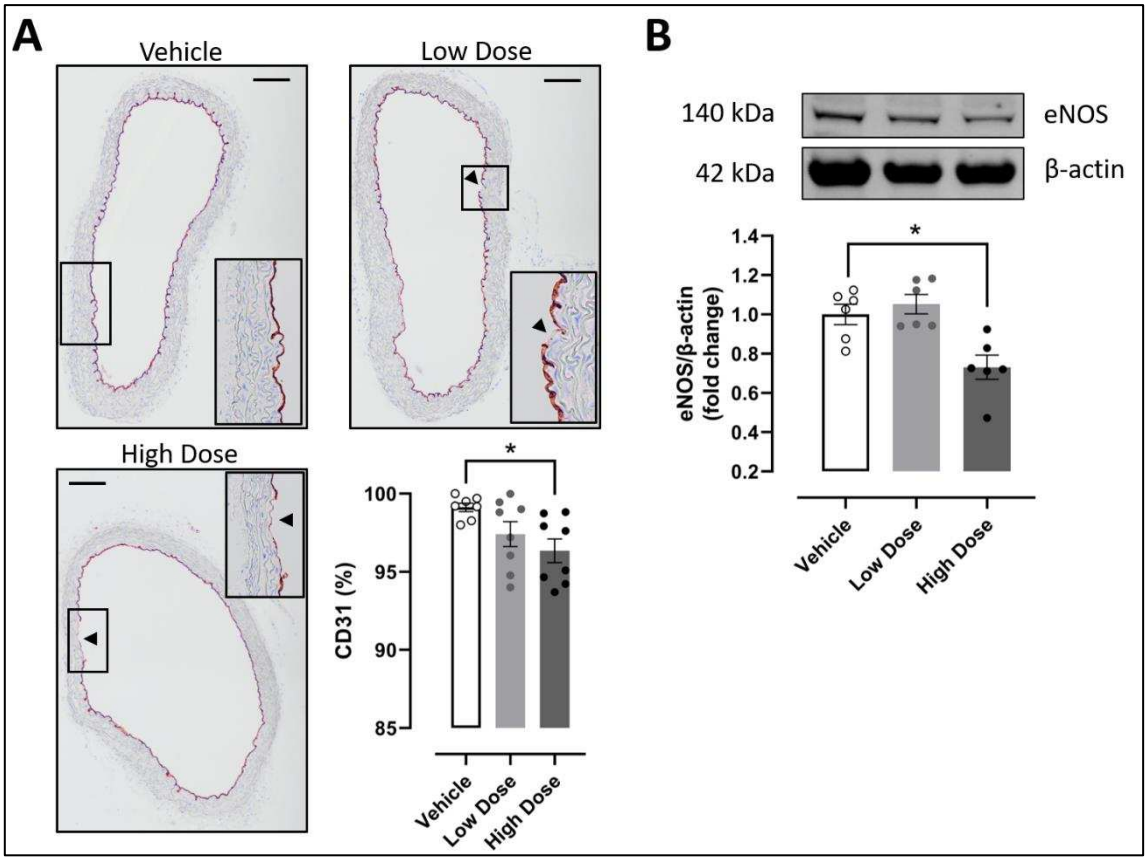

Figure 7: Evaluation of EC layer continuity with CD31 staining and eNOS-expression in mice treated with vehicle, low and high dose of DOX. CD31 staining revealed a significant dose-dependent decrease in EC layer continuity in the high dose group compared to the vehicle (A). In addition, high dose treatment with DOX reduced eNOS-expression (B). Panel A: Black arrows show discontinuity of the endothelial monolayer; For vehicle: n = 7, low dose: n = 8 and high dose: n = 8. Panel B: For vehicle: n = 6, low dose: n = 6 and high dose: n = 6. For A: One-way ANOVA with Dunnett's multiple comparisons test. For B: Kruskal-Wallis with Dunn's multiple comparisons test. * $p < 0.05$; Scale bar: 100 µM (2-column fitting image)

4. DISCUSSION

Arterial stiffness is considered as an important predictor of cardiovascular disease [10]. While clinical studies have demonstrated an increase in arterial stiffness after DOX treatment, the exact mechanism remains elusive [27-30]. Here we present a study where DOX-induced arterial stiffness was investigated in mice, using both *in vivo* and *ex vivo* techniques.

The current study revealed a consistent increase in aaPWV after DOX treatment, while LVEF function remained unaffected. Previously, studies in mice demonstrated LVEF decline after DOX treatment, but these studies used high doses (20-25 mg/kg) [36, 37]. We used lower doses of DOX (8 mg/kg cumulative), since we did not aim to induce severe cardiotoxicity. Body weight and cardiac parameters were not altered after DOX treatment. The

observation of DOX-induced arterial stiffness in the absence of cardiac dysfunction is an important finding. Not only does this indicate that the observed vascular toxicity during DOX treatment was independent of cardiac parameters, but this also suggests that DOX-induced arterial stiffness either precedes DOX-cardiotoxicity, or occurs at lower doses. In both cases, arterial stiffness holds potential as a clinical marker for identifying patients at risk. Additionally, systolic and diastolic blood pressure did not significantly differ, but pulse pressure was elevated in the high dose group, which may point to increased arterial stiffness [38]. The high dose (4 mg/kg) corresponds approximately with 160 mg/m^2 in patients, which is below the maximal recommended dose of 450 mg/m^2 [39, 40]. Furthermore, dosing schedules of DOX for breast cancer [41], non-Hodgkin lymphoma [42] and small cell lung cancer [43] typically involve multiple DOX-infusions every 2 – 3 weeks. The doses used in our preclinical study are also in line with epidemiological studies that have reported accelerated cardiovascular ageing (i.e. increased vascular stiffness), especially in childhood cancer survivors [30].

In patients, regional cfPWV measured by applanation tonometry is the gold standard. In mice, cfPWV measurements are feasible [21], but aaPWV by ultrasound imaging, is more frequently used. Although not the primary objective of our study, we included a comparison between both methods. Bland-Altman analysis showed that aaPWV in mice was consistently higher than cfPWV. aaPWV was more sensitive to detect DOX-induced aortic stiffness *in vivo* in mice, although different timing of the methods and the use of a different anaesthetic do not allow a direct head-to-head comparison. The absolute difference between the aaPWV and cfPWV values can be attributed to variation in geometry and structure of the vessel wall along the arterial tree, which affects the speed of the propagating pulse wave. Previous studies in humans have reported PWV values of 4.4 m/s, 6 m/s and 9 m/s at the aortic root, abdominal aorta and femoral artery, respectively [44, 45]. In this respect, cfPWV represents an integrated average PWV of the different parts of the artery system [44, 45]. In addition, cfPWV measurement depends on determination of the external carotid-femoral distance, which may be prone to a measurement error, particularly in mice [21]. Taken together, these factors might explain the lower cfPWV values and the observation of cfPWV not reaching statistical significance in the high dose group.

The *in vivo* data were confirmed in the *ex vivo* ROTSAC set-up. Aortic rings of high dose-treated mice showed significantly increased aortic stiffness, yet only in the presence of a contractile stimulus (PE). Hence, this finding suggests that a contractile stimulus, provided for example by catecholamines, is essential in the modulation of vascular tone after DOX treatment *in vivo*. Remarkably, in the presence of PE combined with L-NAME, high dose-treated animals showed no pressure-dependency of Ep compared to vehicle-treated animals. More specifically, half of the high dose-treated animals exhibited a decrease in Ep with increasing pressure (data not

shown), resulting in an apparent flattening of the Ep-pressure curve. The exact mechanism remains elusive, although DOX has been shown to induce VSMC death and senescence *in vitro* [46, 47]. Another possible explanation may be the interaction of DOX with the extracellular environment or focal adhesion complexes, which are required for maintaining vascular tonus [48]. Finally, DOX-related structural alterations were evaluated by adding a high dose of DEANO (2 µM), an exogenous NO donor, which relaxes VSMCs and removes vascular tone. In the absence of VSMC tonus, no difference in Ep was observed, which suggests unaltered passive stiffness of the aortic wall. These findings were corroborated by histological stains for elastin and collagen type I, showing no changes in elastin and collagen type I content. Hence, our results point towards active mechanisms contributing to DOX-induced aortic stiffness.

Treatment with the high dose of DOX resulted in increased contraction force in response to PE, an α1-adrenergic receptor agonist. In order to delineate the specific mechanisms involved herein, different aspects of vascular function were further investigated. A dose response of DEANO was used to investigate endothelium-independent relaxation of VSMCs. DEANO causes relaxation of VSMCs through a cyclic guanosine monophosphate (cGMP)-mediated pathway, which results in a reduction in free intracellular Ca^{2+}, thus mediating relaxation of VSMCs [49]. DEANO-induced relaxation did not differ between treatment groups, indicating unaltered guanylate cyclase and cGMP-signalling. This suggests that the sensitivity of VSMCs for NO and the VSMC relaxation capacity remain unaffected after DOX treatment We previously showed that PE causes an increase in intracellular Ca^{2+} through, in part, voltage-gated Ca^{2+}- channels, thus mediating contraction of VSMCs [50]. Therefore, using diltiazem, a voltage-gated Ca^{2+}-channel blocker, can provide useful insight about potential disturbed Ca^{2+}-homeostasis involved in impaired VSMC contraction. Diltiazem-induced relaxation did not differ between the vehicle- and DOX-treated groups. This indicates that Ca^{2+}-influx through voltage-gated calcium channels in VSMCs is not perturbed in response to DOX-administration. Taken together, these findings show that VSMC-specific mechanisms involved in VSMC contraction and relaxation are not impaired. Hence, VSMC function remains intact after DOX treatment.

The endothelial cell layer of the aorta plays a crucial role in regulating VSMC contraction and relaxation [51]. Low levels of basal NO are associated with endothelial dysfunction and, consequently, with increased VSMC contraction, contributing to aortic stiffness [16]. The basal NO index (percentage increase in PE-contraction upon addition of the eNOS blocker L-NAME) provides an estimate about basal NO production and thus is a useful marker for endothelial function. Previous work from our lab has demonstrated that in wild-type C57BL6 mice approximately 80% of maximal contraction (PE + L-NAME) is attributable to basal NO [35]. Contraction force

was higher in the DOX-treated group upon PE-stimulation, but contraction force was similar between all treatment groups after addition of L-NAME. Consequently, the index of basal NO was reduced in DOX-treated animals, indicating that DOX potentially impairs NO production or NO bioavailability.

DOX treatment resulted in reduced CD31 positivity, reflecting gaps in the EC monolayer. This finding indicates that DOX causes EC loss, probably through EC death. In addition, eNOS protein expression was decreased in the high dose group. Both EC loss and reduced eNOS-expression may contribute to the observed decrease in basal NO index, which, in turn, could result in endothelial dysfunction. The observed results are in line with a study of He et al. (2019) in mice, that reported decreased EC viability and reduced eNOS-expression after 3 weeks of DOX treatment (15 mg/kg cumulative) [52]. The authors identified excess ROS-accumulation after DOX treatment as the primary cause of EC death and reduced eNOS expression, which resulted in decreased NO content [52]. DOX-induced ROS generation is mainly caused by the conversion of DOX in a superoxide radical via an intermediate semiquinone structure at the reductase domain of eNOS [53]. Paradoxically, other studies have reported that eNOS expression is upregulated in response to DOX due to ROS-accumulation [31, 54]. Moreover, DOX interferes with eNOS function, resulting in uncoupling of eNOS [31, 54]. In this case, eNOS no longer produces NO, but instead, contributes to superoxide formation, thereby exacerbating ROS-generation. However, these studies were performed using a single high dose of doxorubicin (20 mg/kg) or were performed *in vitro,* which might explain the difference between our results and these other studies.

Similarly, aortic rings of DOX-treated mice exhibited reduced endothelium-dependent relaxation. Previous work from our research group has demonstrated that endothelial dysfunction increases vascular tone and thereby actively augments arterial stiffness [17, 23, 55]. For instance, aortic segments of mice without eNOS expression ($eNOS^{-/-}$) showed no endothelium-dependent relaxation, increased contraction and augmented arterial stiffness [55]. Another recent study demonstrated reduced ACh-induced relaxation after DOX treatment (10 mg/kg cumulative) in mice without altering relaxation in response to an exogenous NO-donor [33]. This is in agreement with our results. However, impaired endothelium-independent relaxation by a NO-donor in mice after DOX treatment (15 mg/kg cumulative) has also been reported [52]. While inactivation of NO by ROS has been proposed as a possible mechanism [56], this concept is not supported by our DEANO relaxation curves, which were identical for the three groups. Possibly, the mechanism of interference with NO signalling depends on the dose of DOX. Our findings suggest that lower doses of DOX (< 15 mg/kg) decrease NO content by decreasing eNOS expression, rather than inactivating NO with excess ROS.

In conclusion, we report a consistent increase in aaPWV in DOX treated mice, which was confirmed *ex vivo*. Moreover, the *ex vivo* ROTSAC and organ bath experiments, revealed that exclusively active components are involved in aortic stiffening in response to DOX. More specifically, DOX impaired endothelial function, resulting in reduced endothelium-dependent relaxation and increased contraction, thereby augmenting arterial stiffness. This endothelial dysfunction could be attributable to EC loss and reduced eNOS-expression. The experimental DOX model and the methods presented in this study, offer the opportunity for further navigating the mechanisms of arterial stiffening in DOX-treated patients.

AUTHOR CONTRIBUTIONS

M.B., G.J., E.V.C., G.D.M., W.M. and P.J.G. conceived and designed the experiments. Data acquisition, analysis, and interpretation were carried out by M.B., K.F., C.N. and P.J.G.. The manuscript was drafted and critically revised by M.B., K.F., C.N., G.J., G.D.M., W.M., E.V.C. and P.J.G. All authors have read and approved the final version of the manuscript.

ACKOWLEDGEMENTS

M.B., K.F. and C.N. are predoctoral fellows of the Fund for Scientific Research (FWO) Flanders [grant number: 1S33720N, 11C6321N and 1S24720N, respectively]. E.V.C. is holder of a senior clinical investigator grant from FWO Flanders [grant number: 1804320N]. Furthermore, the research is supported by a DOCPRO4 grant of the Research Council of the University of Antwerp (ID: 39984) and by the INSPIRE project, which has received funding from the European Union's Horizon 2020 Research and Innovation Program (H2020-MSCA-ITN program, Grant Agreement: No858070).

CONFLICT OF INTEREST

The authors declare that the research was conducted in the absence of any commercial or financial relationships that could be construed as a potential conflict of interest.

REFERENCES

1. Benetos, A., et al., *Pulse pressure: a predictor of long-term cardiovascular mortality in a French male population.* Hypertension, 1997. **30**(6): p. 1410-5.
2. Shirwany, N.A. and M.H. Zou, *Arterial stiffness: a brief review.* Acta Pharmacol Sin, 2010. **31**(10): p. 1267-76.
3. O'Rourke, M.F. and J. Hashimoto, *Mechanical factors in arterial aging: a clinical perspective.* J Am Coll Cardiol, 2007. **50**(1): p. 1-13.
4. Said, M.A., et al., *Relationship of Arterial Stiffness Index and Pulse Pressure With Cardiovascular Disease and Mortality.* J Am Heart Assoc, 2018. **7**(2).
5. Lyle, A.N. and U. Raaz, *Killing Me Unsoftly: Causes and Mechanisms of Arterial Stiffness.* Arterioscler Thromb Vasc Biol, 2017. **37**(2): p. e1-e11.
6. Safar, M.E., et al., *Pulse pressure, arterial stiffness, and end-organ damage.* Curr Hypertens Rep, 2012. **14**(4): p. 339-44.
7. Chae, C.U., et al., *Increased pulse pressure and risk of heart failure in the elderly.* JAMA, 1999. **281**(7): p. 634-9.
8. Sutton-Tyrrell, K., et al., *Elevated aortic pulse wave velocity, a marker of arterial stiffness, predicts cardiovascular events in well-functioning older adults.* Circulation, 2005. **111**(25): p. 3384-90.
9. Mitchell, G.F., et al., *Pulse pressure and risk of new-onset atrial fibrillation.* JAMA, 2007. **297**(7): p. 709-15.
10. Mitchell, G.F., et al., *Sphygmomanometrically determined pulse pressure is a powerful independent predictor of recurrent events after myocardial infarction in patients with impaired left ventricular function. SAVE investigators. Survival and Ventricular Enlargement.* Circulation, 1997. **96**(12): p. 4254-60.
11. Zieman, S.J., V. Melenovsky, and D.A. Kass, *Mechanisms, pathophysiology, and therapy of arterial stiffness.* Arterioscler Thromb Vasc Biol, 2005. **25**(5): p. 932-43.
12. Johnson, C.P., et al., *Age related changes in the tunica media of the vertebral artery: implications for the assessment of vessels injured by trauma.* J Clin Pathol, 2001. **54**(2): p. 139-45.
13. Greenwald, S.E., *Ageing of the conduit arteries.* J Pathol, 2007. **211**(2): p. 157-72.
14. Sehgel, N.L., et al., *Increased vascular smooth muscle cell stiffness: a novel mechanism for aortic stiffness in hypertension.* Am J Physiol Heart Circ Physiol, 2013. **305**(9): p. H1281-7.
15. Bellien, J., et al., *Arterial stiffness is regulated by nitric oxide and endothelium-derived hyperpolarizing factor during changes in blood flow in humans.* Hypertension, 2010. **55**(3): p. 674-80.
16. Fitch, R.M., et al., *Nitric oxide synthase inhibition increases aortic stiffness measured by pulse wave velocity in rats.* Cardiovasc Res, 2001. **51**(2): p. 351-8.
17. Leloup, A.J.A., et al., *Vascular smooth muscle cell contraction and relaxation in the isolated aorta: a critical regulator of large artery compliance.* Physiol Rep, 2019. **7**(4): p. e13934.
18. Laurent, S., et al., *Expert consensus document on arterial stiffness: methodological issues and clinical applications.* Eur Heart J, 2006. **27**(21): p. 2588-605.
19. Hartley, C.J., et al., *Noninvasive determination of pulse-wave velocity in mice.* Am J Physiol, 1997. **273**(1 Pt 2): p. H494-500.
20. Di Lascio, N., et al., *Non-invasive assessment of pulse wave velocity in mice by means of ultrasound images.* Atherosclerosis, 2014. **237**(1): p. 31-7.
21. Leloup, A.J., et al., *Applanation tonometry in mice: a novel noninvasive technique to assess pulse wave velocity and arterial stiffness.* Hypertension, 2014. **64**(1): p. 195-200.
22. Tan, I., et al., *Heart rate dependence of aortic pulse wave velocity at different arterial pressures in rats.* Hypertension, 2012. **60**(2): p. 528-33.

23. Leloup, A.J., et al., *A novel set-up for the ex vivo analysis of mechanical properties of mouse aortic segments stretched at physiological pressure and frequency.* J Physiol, 2016. **594**(21): p. 6105-6115.
24. De Munck, D.G., et al., *Defective autophagy in vascular smooth muscle cells increases passive stiffness of the mouse aortic vessel wall.* Pflugers Arch, 2020. **472**(8): p. 1031-1040.
25. Weiss, R.B., *The anthracyclines: will we ever find a better doxorubicin?* Semin Oncol, 1992. **19**(6): p. 670-86.
26. Renu, K., et al., *Molecular mechanism of doxorubicin-induced cardiomyopathy - An update.* Eur J Pharmacol, 2018. **818**: p. 241-253.
27. Chaosuwannakit, N., et al., *Aortic stiffness increases upon receipt of anthracycline chemotherapy.* J Clin Oncol, 2010. **28**(1): p. 166-72.
28. Parr, S.K., et al., *Anticancer Therapy-Related Increases in Arterial Stiffness: A Systematic Review and Meta-Analysis.* J Am Heart Assoc, 2020. **9**(14): p. e015598.
29. Mozos, I., et al., *Arterial stiffness in hematologic malignancies.* Onco Targets Ther, 2017. **10**: p. 1381-1388.
30. Armstrong, G.T., et al., *Modifiable risk factors and major cardiac events among adult survivors of childhood cancer.* J Clin Oncol, 2013. **31**(29): p. 3673-80.
31. Olukman, M., et al., *Reversal of doxorubicin-induced vascular dysfunction by resveratrol in rat thoracic aorta: Is there a possible role of nitric oxide synthase inhibition?* Anadolu Kardiyol Derg, 2009. **9**(4): p. 260-6.
32. Gibson, N.M., et al., *Doxorubicin-induced vascular dysfunction and its attenuation by exercise preconditioning.* J Cardiovasc Pharmacol, 2013. **62**(4): p. 355-60.
33. Clayton, Z.S., et al., *Doxorubicin-Induced Oxidative Stress and Endothelial Dysfunction in Conduit Arteries Is Prevented by Mitochondrial-Specific Antioxidant Treatment.* JACC CardioOncol, 2020. **2**(3): p. 475-488.
34. Hodjat, M., et al., *Urokinase receptor mediates doxorubicin-induced vascular smooth muscle cell senescence via proteasomal degradation of TRF2.* J Vasc Res, 2013. **50**(2): p. 109-23.
35. van Langen, J., et al., *Selective loss of basal but not receptor-stimulated relaxation by endothelial nitric oxide synthase after isolation of the mouse aorta.* Eur J Pharmacol, 2012. **696**(1-3): p. 111-9.
36. Zhang, S., et al., *Identification of the molecular basis of doxorubicin-induced cardiotoxicity.* Nat Med, 2012. **18**(11): p. 1639-42.
37. Olson, L.E., et al., *Protection from doxorubicin-induced cardiac toxicity in mice with a null allele of carbonyl reductase 1.* Cancer Res, 2003. **63**(20): p. 6602-6.
38. Niiranen, T.J., et al., *Relative Contributions of Pulse Pressure and Arterial Stiffness to Cardiovascular Disease.* Hypertension, 2019. **73**(3): p. 712-717.
39. Zamorano, J.L., et al., *2016 ESC Position Paper on cancer treatments and cardiovascular toxicity developed under the auspices of the ESC Committee for Practice Guidelines: The Task Force for cancer treatments and cardiovascular toxicity of the European Society of Cardiology (ESC).* Eur Heart J, 2016. **37**(36): p. 2768-2801.
40. Swain, S.M., F.S. Whaley, and M.S. Ewer, *Congestive heart failure in patients treated with doxorubicin: a retrospective analysis of three trials.* Cancer, 2003. **97**(11): p. 2869-79.
41. Bull, J.M., et al., *A randomized comparative trial of adriamycin versus methotrexate in combination drug therapy.* Cancer, 1978. **41**(5): p. 1649-57.
42. Geisler, C.H., et al., *Long-term progression-free survival of mantle cell lymphoma after intensive front-line immunochemotherapy with in vivo-purged stem cell rescue: a nonrandomized phase 2 multicenter study by the Nordic Lymphoma Group.* Blood, 2008. **112**(7): p. 2687-93.
43. von Pawel, J., et al., *Topotecan versus cyclophosphamide, doxorubicin, and vincristine for the treatment of recurrent small-cell lung cancer.* J Clin Oncol, 1999. **17**(2): p. 658-67.

44. Nichols, W.W. and D.A. McDonald, *Wave-velocity in the proximal aorta.* Med Biol Eng, 1972. **10**(3): p. 327-35.
45. Latham, R.D., et al., *Regional wave travel and reflections along the human aorta: a study with six simultaneous micromanometric pressures.* Circulation, 1985. **72**(6): p. 1257-69.
46. Murata, T., et al., *Chronic effect of doxorubicin on vascular endothelium assessed by organ culture study.* Life Sci, 2001. **69**(22): p. 2685-95.
47. Sung, J.Y., et al., *Interaction between mTOR pathway inhibition and autophagy induction attenuates adriamycin-induced vascular smooth muscle cell senescence through decreased expressions of p53/p21/p16.* Exp Gerontol, 2018. **109**: p. 51-58.
48. Hong, Z., et al., *Vascular smooth muscle cell stiffness and adhesion to collagen I modified by vasoactive agonists.* PLoS One, 2015. **10**(3): p. e0119533.
49. Carvajal, J.A., et al., *Molecular mechanism of cGMP-mediated smooth muscle relaxation.* J Cell Physiol, 2000. **184**(3): p. 409-20.
50. Fransen, P., et al., *Dissecting out the complex Ca2+-mediated phenylephrine-induced contractions of mouse aortic segments.* PLoS One, 2015. **10**(3): p. e0121634.
51. Luscher, T.F. and F.C. Tanner, *Endothelial regulation of vascular tone and growth.* Am J Hypertens, 1993. **6**(7 Pt 2): p. 283S-293S.
52. He, H., et al., *Doxorubicin Induces Endotheliotoxicity and Mitochondrial Dysfunction via ROS/eNOS/NO Pathway.* Front Pharmacol, 2019. **10**: p. 1531.
53. Vasquez-Vivar, J., et al., *Endothelial nitric oxide synthase-dependent superoxide generation from adriamycin.* Biochemistry, 1997. **36**(38): p. 11293-7.
54. Kalivendi, S.V., et al., *Doxorubicin-induced apoptosis is associated with increased transcription of endothelial nitric-oxide synthase. Effect of antiapoptotic antioxidants and calcium.* J Biol Chem, 2001. **276**(50): p. 47266-76.
55. Leloup, A.J.A., et al., *Ex vivo aortic stiffness in mice with different eNOS activity.* Am J Physiol Heart Circ Physiol, 2020. **318**(5): p. H1233-H1244.
56. Vaziri, N.D., K. Liang, and Y. Ding, *Increased nitric oxide inactivation by reactive oxygen species in lead-induced hypertension.* Kidney Int, 1999. **56**(4): p. 1492-8.

SUPPLEMENTARY FIGURES

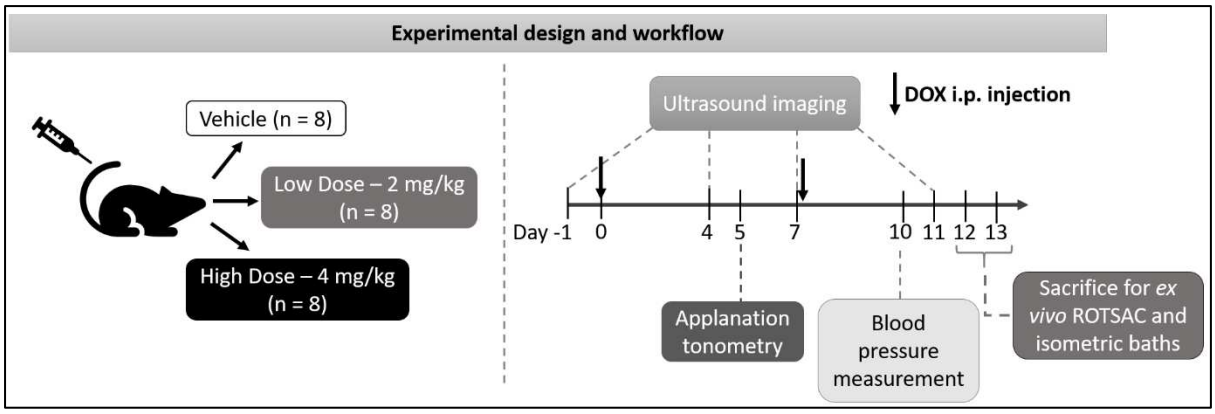

Supplementary figure 1: Experimental design and workflow. Male C57BL/6J mice were randomly divided into three groups: a vehicle (n = 8), a low dose (n = 8) and a high dose group (n = 8). The low and high dose groups received an intraperitoneal injection of 2 and 4 mg DOX/kg, respectively, once per week for a total of two weeks. Ultrasound imaging for determination of aaPWV was performed at day -1 (baseline) and 4, 7 and 11 days after the start of DOX treatment for all groups. Applanation tonometry for determination of cfPWV was only performed at 5 days after the start of treatment. A blood pressure measurement was performed at day 10 (with two training days at day 8 and 9). Mice were sacrificed and the aorta was removed for *ex vivo* ROTSAC and isometric organ bath evaluation at 12 or 13 days after initiating DOX treatment.

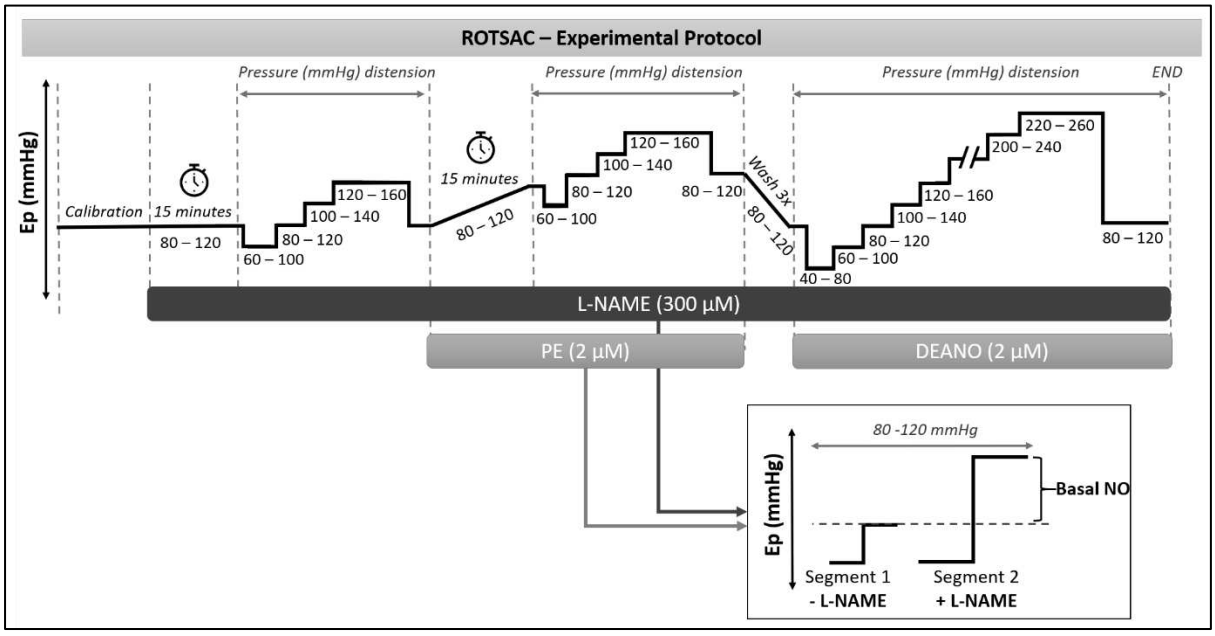

Supplementary figure 2: Experimental protocol for aortic stiffness evaluation in ROTSAC set-up. Following calibration, Nω-nitro-L-arginine methyl ester (L-NAME, 300 µM) was added to one segment to inhibit endothelial nitric oxide synthase (eNOS) activity to investigate the basal NO index. After 15 minutes, Ep was calculated for each pressure (from 60 - 100 mmHg to 120 - 160 mmHg). In order to investigate the active contribution of VSMCs to DOX-induced aortic stiffness, phenylephrine (PE, 2 µM) was subsequently added to the organ bath, followed by 15 minutes of incubation while keeping pressure constant at 80-120 mmHg. PE is a selective agonist of α1-adrenergic receptors on VSMCs and thereby initiates IP-3 mediated contraction. After 15 minutes, Ep was calculated for each pressure (from 60 - 100 mmHg to 120 - 160 mmHg). After washing 3x with Krebs, diethylamine NONOate (DEANO, 2 µM) was added to the organ bath and Ep was calculated for each pressure (from 40 - 80 mmHg to 220 - 260 mmHg). DEANO is an exogenous NO-donor and induces endothelium-independent relaxation of VSMCs, thereby excluding VSMC tonus. This allows examination of the potential contribution of passive elements to DOX-induced aortic stiffness.

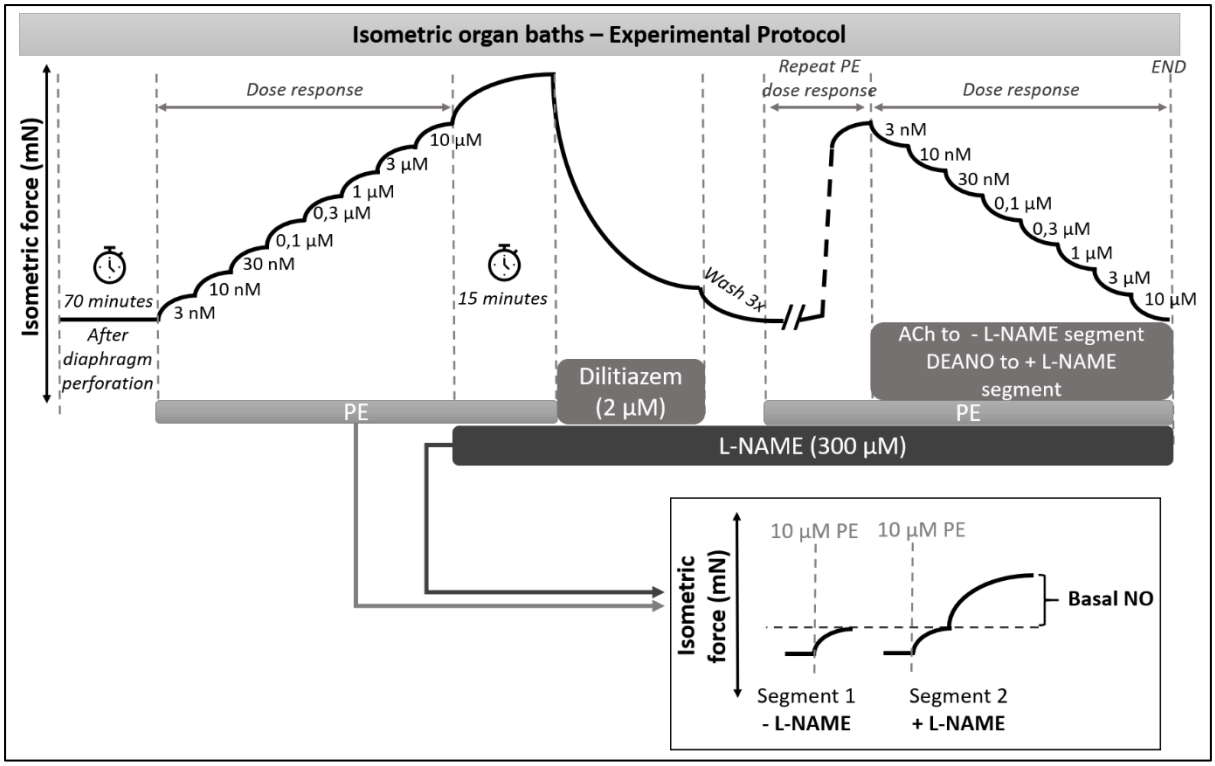

Supplementary figure 3: Experimental protocol for vascular reactivity assessment in isometric organ baths. First, increasing doses of PE were added to all segments with 2 minute intervals to investigate contractility force, followed by addition of L-NAME (300 µM) to 1 segment. Next, diltiazem (2 µM) was added to the organ bath to investigate the role of calcium channels in DOX-induced arterial stiffness. Diltiazem is a calcium-channel blocker, which inhibits calcium influx into the intracellular environment, thereby inhibiting contraction and inducing relaxation. After washing 3x with Krebs, the PE-dose response was repeated, followed by addition of increasing doses of acetylcholine (ACh) to the L-NAME-untreated segment and increasing doses of DEANO to the L-NAME-treated segment. ACh is a neurotransmitter that, when it binds to corresponding receptors on the endothelium, induces relaxation of VSMCs. This allows examination of endothelial-dependent VSMC relaxation and endothelial function in general.